Magnetic Design Optimization approach using Design of Experiments with Evolutionary Computing

P. Di Barba[1], F. Dughiero[2], M. Forzan[2], and E. Sieni[2]

[1]Department of Electrical, Computer and Biomedical Engineering, University of Pavia, 27100 Pavia, Italy
[2]Department of Industrial Engineering, University of Padova, 35131 Padova, Italy

A new optimization method, combining design of experiments with evolutionary computing, is proposed: it handles a set of design variables, the size of which changes during the process: initially, most sensitive variables are activated; subsequently, the whole set of variables is activated. The optimal synthesis of a magnetic field for magneto-fluid treatment is considered as the case study.

Index Terms— **Evolutionary computing, multiobjective optimal design, sensitivity analysis, finite elements, magnetic field synthesis**

I. Introduction

When tackling problems of optimal shape design in magnetics, characterized by Finite Elements (FE) field analyses for solving the associated direct problem, the so-called parametric approach is normally adopted: a set of many design variables, defining the unknown shape of the device to synthesize, is searched for, usually exploiting algorithms of evolutionary computing. In particular, in multi-objective problems, the search for the Pareto-optimal front of the problem is based on popular algorithms like *e.g.* Non-Dominated Genetic Algorithm (NSGA) or Multi Objective Particle Swarm Optimization (MOPSO) [1]–[9]. When the dimensionality of the design problem, mainly dictated by the number of design variables, is high, a combinatorial increase of feasible design points occurs: in case, cost-effective procedures of optimization can be implemented exploiting *e.g.* surrogate models, *i.e.* identifying response surfaces that replace the objective functions at a lower cost [10]–[12]. Alternatively, one might think of subdividing the design variable set in *e.g.* two subsets, in such a way that the first part of the optimization is driven by the most sensitive variables, in order to approach fast the region of Pareto-optimal solutions, and then switching to the full set of variables, in order to focus on the details of the search region. Progressively enhancing the design variable set emulates what happens in the real-life behavior of a device designer. In fact, the rationale behind the proposed method is based on the 'natural' process of design undertaken by the human being: first, the most influential variables are modified to substantially improve the design criterion, next marginal improvements are searched for by 'squeezing' least sensitive variables.

II. Proposed Optimization Method

The proposed optimization method combines Design Of Experiments (DOE) [13] with NSGA [4], and acts on a set of design variables, the size of which changes during the optimization process. The SV-NSGA-DOE (SV, switched variables) algorithm works as shown in Fig 1. At the beginning the whole set of design variables is defined with relevant intervals. Initially, the DOE analysis is used to define the subset of design variables that are more sensible within the prescribed intervals. To this end, exploiting Placket-Burmann tables [13], a cost-effective evaluation of sensitivity is performed: a number N_{DOE} of FE analyses makes it possible to approximate the sensitivity S_{xi} of each out of N_V design variables. Then, the average sensitivity, S_m, is computed:

$$S_m = \frac{1}{N_V}\sum_{i=1}^{N_V} S_{x,i} \tag{1}$$

The most sensitive design variables are defined as those for which $S_{x,i} > S_m$, i=1,..N_V. This way, a reduced set of design variables is activated. The sensitivity evaluation (1) takes place only once, before the NSGA-based optimization is started. In fact, the first approximation of the Pareto front is obtained by applying NSGA-II just on the reduced set of design variables; meanwhile, the complementary subset of design variables are 'frozen' to their initial value. After a number of iterations, according to the criterion explained in the following, it is decided to make a switch: the full set of design variables is eventually activated. Therefore, NSGA optimization is performed in two steps (Fig. 1): in the former only the reduced set of most sensitive design variables is considered, while in the latter the full set of design variables is considered. N_{pop} individuals are selected in the initial population, which N_{DOE} individuals used for the DOE analysis are added to. Therefore, the initial population contains N_{DOE} + N_{pop} individuals. A first selection, ruled by non-dominated sorting, reduces the population size to N_{pop}. At each iteration the stopping criterion is evaluated: if it is fulfilled, the algorithm 'switches' and all the design variables are activated in the optimization procedure. The optimization handling the full set of design variables ends when the same stopping criterion is fulfilled.

Manuscript received ….., 2015; revised ……, 2015 and ….., 2015; accepted ….., 2015. Date of publication July 10, 2015; date of current version July 31, 2015. Corresponding author: E. Sieni (e-mail: elisabetta.sieni@unipd.it).

Color versions of one or more of the figures in this paper are available online at http://ieeexplore.ieee.org.

Digital Object Identifier (inserted by IEEE).

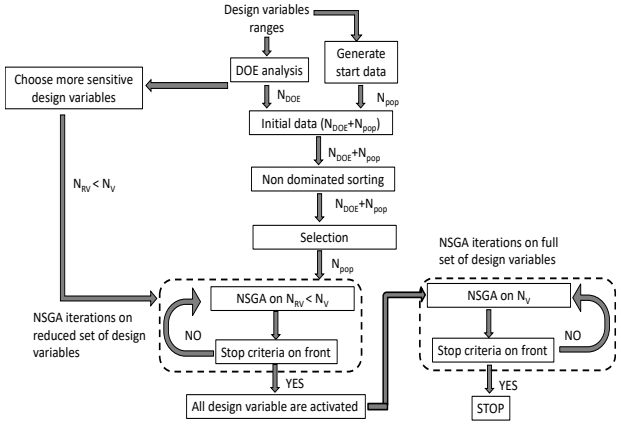

Fig. 1. Flow chart of SV-NSGA-DOE algorithm.

The NSGA algorithm generally stops when the maximum number of iteration is achieved. In this work, an automatic stopping criterion, based on the evaluation of the front displacement, is implemented. In particular, in the chromosome of the *h-th* iteration the distance of each individual from the origin of the objective space or from utopia point, $d_j(h)$ $j=1,\ldots,N_{pop}$, is computed. Then, the average distance, $d_m(h)$, is evaluated as:

$$d_m(h) = \frac{1}{N_{pop}} \sum_{j=1}^{N_{pop}} d_j(h) \tag{2}$$

This average distance is compared with the one at the previous generation, $d_m(h-1)$. If the relative difference is lower than a prescribed threshold, $d_{\%,th}$ (*e.g.* 1%), the front is considered to be stationary and the NSGA can either 'switch' to the full set of design variables (first step) or stop (second step). In practice, the switch or stop event is decided by averaging some, e.g. 10, percentage differences, $d_{\%}(h)$.

III. Case Study: Power Inductor for Magnetic Nanoparticle Heating

A. Direct problem

Fig. 2(a) shows the cross section of the axi-symmetric geometry of the device used to test NPs in cell culture for Magnetic Fluid Hyperthermia applications [14]–[16]. The Petri dish is placed in a thermally insulated box where a water flow keeps the temperature of the system at 37°C. The magnetic field device is a two-turn inductor with a radius of 83 mm with five ferrite blocks placed as in Fig. 2(a) in order to concentrate the magnetic flux lines [17], [18]. The magnetic field analysis problem, based on the **A**-V formulation, is solved in time-harmonics conditions using a FE code [19]. The inductor is to be supplied by means of a voltage generator, applying 600 V_{rms} at 350 kHz. A typical FE mesh exhibits 23,000 nodes and 13,000 elements.

The magnetic problem is solved in terms of the phasor of magnetic vector potential, ***A***, and electric scalar potential, V. When the Coulomb gauge is applied on the magnetic vector potential, i.e. $\nabla \cdot \boldsymbol{A} = 0$, the following two coupled equations are solved [20]:

$$\nabla \times \mu^{-1} \nabla \times \boldsymbol{A} + j\omega\mu\rho^{-1}\boldsymbol{A} = -\rho^{-1}\nabla V \tag{3}$$

$$\nabla \cdot \rho^{-1}(j\omega\mu \boldsymbol{A} + \nabla V) = 0 \tag{4}$$

subject to suitable boundary conditions, where ρ and μ are the material resistivity and permeability, respectively and ω the field pulsation. Fig. 2 (b) shows typical magnetic field lines.
The problem has been studied assuming a voltage supply of 600 V_{rms} for the inductor, which is an acceptable value for a generator rating a power of 10 kW in the frequency range of 150-400 kHz [18].

B. Inverse problem

The inverse problem is characterized by seven design variables that define the inductor geometry, namely: vertical positions (d_0, d_1, d_2) of the ferrite rings on the top, vertical size H_S and turn step ST of the inductor turns, sizes (L_F, H_{FS}) of the ferrite block at the bottom, respectively. The design variables range is reported in Table I.

TABLE I: DESIGN VARIABLES RANGE IN [MM].

	d_0	d_1	d_2	Hs	ST	L_F	H_{FS}
min	1.0	1.0	1.0	5.0	1.0	20.0	5.0
max	30.0	30.0	30.0	50.0	20.0	75.0	20.0

The aim of the optimization problem is twofold: to minimize the inhomogeneity (f_1) of the magnetic field, H, in the Petri dish with a tolerance interval of ΔH = ±10 A/m, and to minimize the inverse (f_2) of the average magnetic field strength in the Petri dish bottom. The inhomogeneity has been computed according to the proximity criterion. This criterion takes into account the number of grid points where the magnetic field strength exceeds a tolerance band ΔH around a given reference value. In practice, the lowest number of points falling outside the tolerance band is searched for [21]–[23].

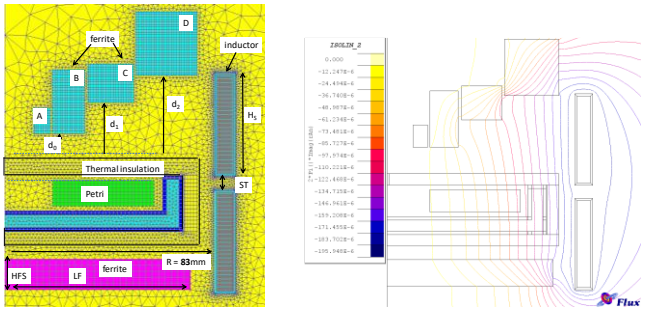

(a) (b)

Fig. 2. (a) Model geometry, mesh, design variables. (b) Magnetic flux lines.

IV. Results

Fig. 3 and 4 shows the approximated Pareto fronts obtained starting from the same initial population of N_{pop} individuals and applying one out of the following three methods:

a. NSGA-II algorithm in the standard version (results referred as #_NSGA);
b. SV-NSGA-DOE, the modified NSGA algorithm including the switching strategy (results referred as #_SV);
c. NSGA-II algorithm in the standard version in which

the initial population incorporates also the DOE-evaluated individuals (named NSGA-DOE, results referred as #_DOE).

In the case study here considered, three design variables are selected as the most sensitive in the reduced set (d_2, ST and HFS in Fig 2). In Fig. 3 it appears that the Pareto front obtained using the proposed SV-NSGA-DOE algorithm is broader than the one found via a standard NSGA-II algorithm. Fig. 4 compares the approximated Pareto fronts obtained by means of classical implementation of NSGA-II algorithm starting from the population including N_{pop} individuals, or starting from the population including also the individuals generated by the DOE analysis. It turns out to be that incorporating the extra individuals used in the initial DOE analysis contributes to enhance the approximated Pareto front. Moreover, it can be noted that the solutions obtained by means of reduced design variable set are located at the ends of the Pareto front.

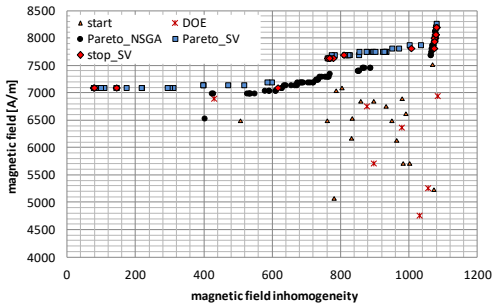

Fig. 3. Pareto fronts obtained applying methods a and b with the same initial population (start). Pareto_#= individuals on Pareto front, DOE= individuals of the DOE analysis, stop_SV= individuals at switching iteration using b.

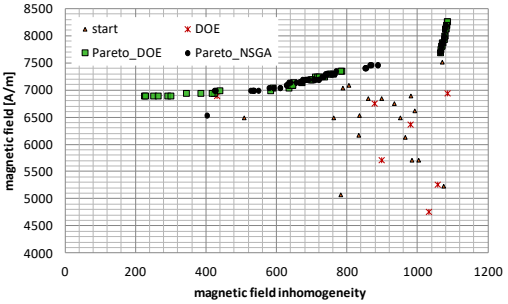

Fig. 4. Pareto fronts obtained applying methods a and c.

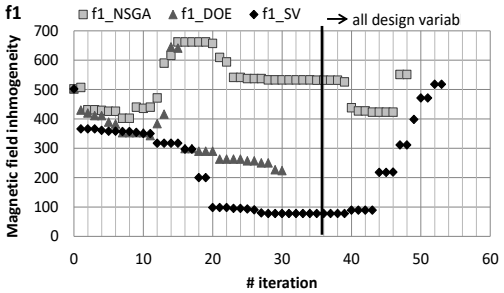

Fig. 5. History of the f1 objective function: the switch line from reduced to full set of design variables is shown.

In Fig. 5 the evolution of the f_1 objective function is shown, considering at each iteration the best out of N_{pop} values. It can be noted that substantial function variations take place both before and after the switch of design variables.

Considering the automatic stop criterion (2), it turns out to be that NSGA stops after 30 iterations, NSGA-DOE after 48, and SV-NSGA-DOE after 53 (the design variables switch occurs after 36 iterations). Table II reports a selection of solutions computed nearby the switching iteration: between iterations 34 and 35 only three out of seven design variables were active and underwent modifications (in bold); in contrast, between iterations 35 and 36 all the seven design variables were activated.

TABLE II: SELECTION OF INDIVIDUALS (DESIGN VARIABLES IN [MM], OBJECTIVE FUNCTIONS F_1 DIMENSIONLESS AND F_2 IN [A/M]) BEFORE SWITCHING (BS) AND AT SWITCHING (S).

#it	d_0	d_1	d_2	Hs	ST	L_F	H_{FS}	f_1	f_2
34_{BS}	1.21	14.68	**28.81**	35.11	**17.58**	49.11	**19.99**	1081	8197
35_{BS}	1.21	14.68	**28.71**	35.11	**17.52**	49.11	**20.00**	1081	8197
35_{BS}	1.00	30.00	26.80	50.00	3.19	75.00	12.95	1075	7937
36_S	1.01	29.29	26.70	50.00	1.00	74.04	13.30	1075	8000
35_{BS}	1.21	14.68	28.82	35.11	17.60	49.11	20.00	1081	8197
36_S	1.22	14.68	28.67	35.15	17.54	48.99	19.94	1081	8197
35_{BS}	1.00	30.00	30.00	50.00	1.36	5.00	6.73	1077	8000
36_S	1.00	29.79	26.79	49.99	3.22	74.98	12.93	1075	7937

Fig. 6 shows the three geometries (data reported in Table III) that exhibit the lowest magnetic field inhomogeneity for each optimization strategies, NSGA-II, SV-NSGA-DOE and NSGA-DOE**.** Considering the tolerance interval of the proximity criterion (ΔH = ±10 A/m) and the current average value of the magnetic field strength, H_{av}, the inhomogeneity is computed as the ratio of the tolerance band, ΔH, to the average magnetic field strength, H_{av} ; its value is close to 0.3% for all the three solutions shown in Fig. 6. Alternatively, after evaluating the inhomogeneity as the ratio of the largest discrepancy of magnetic field in the Petri dish bottom to H_{av}, it turns out to be 1.9 %, 0.5 % and 1.5 % for case a, b and c, respectively. It appears that the geometries of the device are different; moreover, the switched variable algorithm shows a lower inhomogeneity for higher magnetic field strength (case b: higher than 7000 A/m; case a and c: close to 6500 and 6900 A/m, respectively).

TABLE III: BEST SOLUTIONS ON THE PARETO FRONT. DESIGN VARIABLES [MM], OBJECTIVE FUNCTIONS F_1 DIMENSIONLESS AND F_2 [A/M].

	d_0	d_1	d_2	Hs	ST	L_F	H_{FS}	f_1	f_2
a	26.8	23.3	23.6	27.0	18.8	44.9	7.5	402	6536
b	30.0	30.0	30.0	50.0	1.0	75.0	6.6	78	7092
c	2.4	4.8	1.0	49.4	11.0	53.1	8.3	224	6897

Figs. 7 and 8 show the approximated Pareto fronts obtained starting from a different initial population. The individuals evaluated using DOE marginally improve the front, but the best improvement is obtained by means of the design variable switching strategy. Considering the automatic stop criterion (2), it turns out to be that NSGA stops after 16 iterations, NSGA-DOE after 23, and SV-NSGA-DOE after 42; the design variable switch occurs after 20 iterations. Fig. 9 shows the three geometries (data in Table IV) that exhibit the lowest magnetic field inhomogeneity, obtained for each optimization strategies: NSGA-II, SV-NSGA-DOE and NSGA-DOE. Again, it appears that the optimal geometries of the device are different.

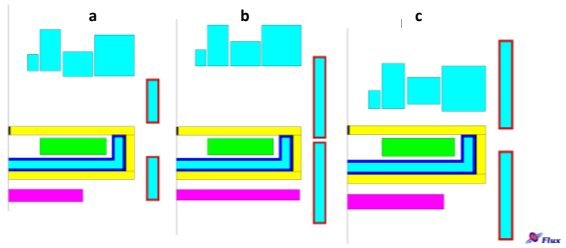

Fig. 6 Optimal geometries obtained using: a= NSGA-II, b= SV-NSGA-DOE and c=NSGA-DOE. Case 1.

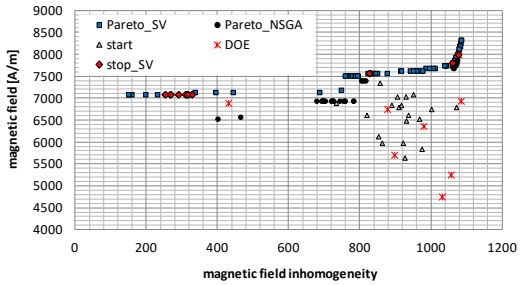

Fig. 7. Pareto fronts obtained starting from the same initial population (start) and applying methods a and b.

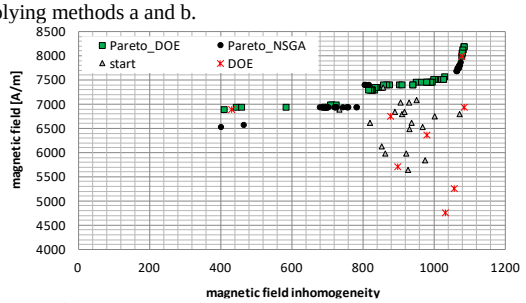

Fig. 8. Pareto fronts obtained from the same initial population (start) with the methods a and c.

TABLE IV: BEST SOLUTIONS ON THE PARETO FRONT. DESIGN VARIABLES [MM], OBJECTIVE FUNCTIONS F_1 DIMENSIONLESS AND F_2 [A/M].

	d_0	d_1	d_2	Hs	ST	L_F	H_{FS}	f_1	f_2
a	25.5	24.2	23.6	27.8	19.6	45.9	7.1	400	6536
b	28.5	30.0	30.0	50.0	4.3	75.0	17.5	149	7092
c	30.0	29.5	29.6	49.9	19.9	74.8	20.0	409	6897

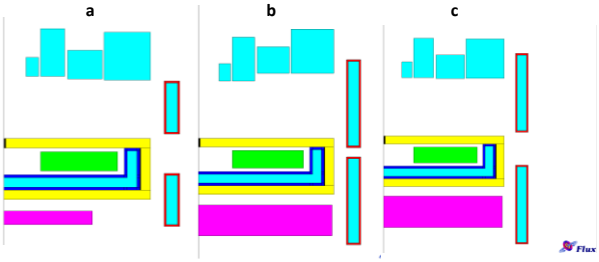

Fig. 9 Optimal geometries obtained using: a= NSGA-II, B= SV-NSGA-DOE and c=NSGA-DOE. Case 2.

Comparing results with the ones of the previous case, it appears that in the case of NSGA-II algorithm the better solution in terms of lowest inhomogeneity of magnetic field is close to the one obtained in the previous case starting from a different initial population and reported in Fig. 6. Moreover, the geometry of the solution obtained via NSGA-DOE is different with respect to the one of the previous case and reported in Fig. 6. Finally, the geometry of the solutions obtained using SV-NSGA-DOE exhibits a dependence on the initial population.

V. CONCLUSIONS

The proposed algorithm, based on the automatic switch of design variables, has proven to be able to improve the approximated Pareto front with respect to the one obtained using standard NSGA strategy.

REFERENCES

[1] K. Deb, *Multi-objective optimization using evolutionary algorithms*, 1st ed. Chichester ; New York: John Wiley & Sons, 2001.

[2] K. Deb, A. Pratap, S. Agarwal, T. Meyarivan, "A fast and elitist multiobjective genetic algorithm: NSGA-II", *Evol. Comput. IEEE Trans. On*, vol. 6, n. 2, pp. 182–197, 2002.

[3] A. Nourbakhsh, H. Safikhani, S. Derakhshan, "The comparison of multi-objective particle swarm optimization and NSGA II algorithm: applications in centrifugal pumps", *Eng. Optim.*, vol. 43, n. 10, pp. 1095–1113, 2011.

[4] P. Di Barba, *Multiobjective shape design in electricity and magnetism*. Doredrecht ; New York: Springer, 2010.

[5] J. Kennedy, R. Eberhart, "Particle swarm optimization", *Neural Netw. 1995 Proc. IEEE Int. Conf. On*, vol. 4, pp. 1942–1948 vol.4, 1995.

[6] F. Riganti Fulginei, A. Salvini, "The Flock of Starlings Optimization: Influence of Topological Rules on the Collective Behavior of Swarm Intelligence", in *Computational Methods for the Innovative Design of Electrical Devices*, vol. 327, pp. 129–145, 2011.

[7] E. Zitzler, L. Thiele, "Multiobjective evolutionary algorithms: a comparative case study and the strength Pareto approach", *Evol. Comput. IEEE Trans. On*, vol. 3, n. 4, pp. 257–271, 1999.

[8] S. Karakostas, "Multi-objective optimization in spatial planning: Improving the effectiveness of multi-objective evolutionary algorithms (non-dominated sorting genetic algorithm II)", *Eng. Optim.*, pp. 1–21, 2014.

[9] P. Di Barba, F. Dughiero, E. Sieni, "Field synthesis for the optimal treatment planning in Magnetic Fluid Hyperthermia", *Arch. Electr. Eng.*, vol. 61, n. 1, pp. 57–67, 2012.

[10] R. H. Myers, *Response surface methodology: process and product optimization using designed experiments*, 3rd ed. Hoboken, N.J: Wiley, 2009.

[11] D. C. Montgomery, *Design and analysis of experiments*, Eighth edition. Hoboken, NJ: John Wiley & Sons, Inc, 2013.

[12] C. M. Anderson-Cook, C. M. Borror, D. C. Montgomery, "Response surface design evaluation and comparison", *J. Stat. Plan. Inference*, vol. 139, n. 2, pp. 629–641, 2009.

[13] R. L. Plackett, J. P. Burman, "The Design of Optimum Multifactorial Experiments", *Biometrika*, vol. 33, n. 4, pp. 305–325, 1946.

[14] P. D. Di Barba, F. Dughiero, E. Sieni, "Magnetic Field Synthesis in the Design of Inductors for Magnetic Fluid Hyperthermia", *Magn. IEEE Trans. On*, vol. 46, n. 8, pp. 2931–2934, 2010.

[15] P. Di Barba, F. Dughiero, E. Sieni, A. Candeo, "Coupled Field Synthesis in Magnetic Fluid Hyperthermia", *Magn. IEEE Trans.*, vol. 47, n. 5, pp. 914–917, 2011.

[16] P. Di Barba, F. Dughiero, E. Sieni, "Synthesizing distributions of magnetic nanoparticles for clinical hyperthermia", *Magn. IEEE Trans. On*, vol. 48, n. 2, pp. 263–266, 2012.

[17] P. Di Barba, M. Forzan, E. Sieni, F. Dughiero, "Sensitivity-based optimal shape design of induction-heating devices", *IET Sci. Meas. Technol.*, 2015.

[18] R. Bertani, F. Ceretta, P. Di Barba, M. Forzan, F. Dughiero, R. Michelin, P. Sgarbossa, E. Sieni, Federico Spizzo, "Optimal Inductor design for nanofluid heating characterisation", *Eng. Comput.*, in press.

[19] FLUX, "(CEDRAT): www.cedrat.com/software/flux/flux.html". .

[20] P. Di Barba, A. Savini, . Wiak, *Field models in electricity and magnetism*. [Dordrecht]: Springer, 2008.

[21] P. Di Barba, F. Dughiero, M. Forzan, E. Sieni, "A paretian approach to optimal design with uncertainties: application in induction heating", *Magn. IEEE Trans*, vol. 50, n. 2, pp. 917–920, 2014.

[22] P. Di Barba, M. Forzan, E. Sieni, "Multi-objective design of a power inductor: a benchmark problem of inverse induction heating", *COMPEL*, vol. 33, n. 6, pp. 1990–2005, 2014.

[23] P. Di Barba, M. Forzan, E. Sieni, "Multiobjective design optimization of an induction heating device: a benchmark problem", *Int. J. Appl. Electromagn. Mech.*, vol. 47, pp. 1003–1013, 2015.